

APPENDIX C

CEUS AND WUS STRONG GROUND MOTIONS AT ROCK SITES

1 INTRODUCTION

Recent observations of both small and intermediate magnitude earthquakes which have occurred in central and eastern North America have shown larger peak accelerations as well as high frequency spectral content (≥ 5 to 10 Hz) than would be expected based on recordings in western North America, principally California (Brady et al., 1981; Chang, 1983; Borchardt, 1986; Wesson and Nicholson, 1986; Weichert et al., 1982; 1986; Munro and Weichert, 1989; Silva and Darragh, 1995). In addition to these observations at high frequencies, intermediate magnitude ($M \approx 6.2$) earthquakes have shown an opposite trend at intermediate and low frequencies (below about 2 Hz), having lower motions than comparable (M , distance, and site condition) WUS recordings would suggest (Boore and Atkinson, 1992; Atkinson, 1993; Silva and Darragh, 1995). This latter observation, in terms of strong ground motions, is principally limited to the 1988 M 5.8 Saguenay, Canada earthquake but is supported by inferences from intensity data (Atkinson, 1993), regional seismograms ($D \approx 1,000$ km) of early instrumental recordings in eastern North America (Atkinson and Chen, 1997), and teleseismic data of worldwide intraplate earthquakes (Boatwright and Choy, 1992).

The differences in high frequency spectral content between WUS and CEUS strong ground motions especially for very stiff (rock) site conditions, is pervasive and reasonably well understood (Boore and Atkinson, 1987; Boore et al., 1992; EPRI, 1993; Silva and Darragh, 1995; Atkinson, 1996). As a result, the uncertainty in whether or not future earthquakes occurring in the CEUS will have high frequency spectral characteristics at hard rock sites distinctly different than the WUS

APPENDIX C

(California) experience is considered low. Conversely, the differences in low frequency spectral content between WUS and CEUS strong ground motions is neither well constrained through direct observations nor understood physically. The following discussion is intended to illustrate the differences between WUS and CEUS rock site motions and to suggest the physical bases for the differences.

2 CEUS AND WUS STRONG GROUND MOTIONS AT ROCK SITES

Observations of strong ground motion due to small magnitude earthquakes occurring in eastern North America, although not causing damage to engineered structures, have shown considerably higher peak accelerations than would have been expected based upon WUS experience (Brady et al., 1981; Chang, 1983; Wesson and Nicholson, 1986; Weichert et al., 1982; 1986; Munro and Weichert, 1989). In addition to the relatively higher peak accelerations associated with these CEUS events, response spectral ordinates appear richer in high frequency energy, particularly for frequencies exceeding about 10 Hz (Brady et al., 1981; Borchardt, 1986).

It has been known for some time that ground motion for CEUS attenuate less rapidly with distance than ground motion in WUS for events of similar moment magnitudes and source depths (Nuttli, 1981; EPRI, 1993; Atkinson and Boore 1995). The difference in attenuation rate has been attributed to the higher absorptive characteristics generally present in the crust and upper mantle beneath WUS as compared to CEUS (Nuttli, 1981; Herrmann and Nuttli, 1982; Singh and Herrmann, 1983; Boore and Atkinson, 1987; Toro and McGuire, 1987; Frankel et al., 1990; Hanks and Johnston, 1992; EPRI, 1993; Frankel, 1994; Benz et al., 1997). These differences may be a consequence of active plate margin tectonics as opposed to conditions representative of a stable

APPENDIX C

continental interior.

For close-in recordings, where the propagation path is short (< 20 to 30 km), the difference in crustal attenuation between WUS and CEUS was thought to have a minimal effect and strong ground motion was expected to be comparable in the two tectonic environments (Campbell, 1981, 1986; Kimball, 1983). However, close-in (< 20 km) strong motion recordings of the 1978 Monticello, South Carolina earthquakes with moment magnitudes of approximately 3 produced a maximum peak-horizontal acceleration of 0.25g (Brady et al., 1981; Mork and Brady, 1981) and the 1986 Painesville, Ohio earthquake with a magnitude of 5.0 (m_{Lg}) produced a peak acceleration of nearly 0.20g at an 18 km epicentral distance (Wesson and Nicholson, 1986); both values are significantly higher than would be expected for earthquakes of similar magnitude and distance in WUS. Recordings from both of these earthquakes also show unexpected high-frequency energy content in the response spectra compared to similar magnitude WUS recordings (Silva and Darragh, 1995).

Other sources of data also indicate that CEUS ground motions, recorded at rock or very shallow soil sites, are richer in high-frequency energy relative to analogous WUS ground motions. These include aftershocks of the 1982 Miramichi, New Brunswick earthquake (Cranswick et al., 1985), the 1982 Enola, Arkansas swarm (Haar et al., 1984), aftershocks of the 1986 Painesville, Ohio event (Borcherdt, 1986), the 1985 Nahanni earthquakes (Weichert et al., 1986), the 1982 New Hampshire earthquake (Chang, 1983), and the **M** 5.8 1988 Saguenay earthquakes (Boore and Atkinson, 1992). The trends shown in these CEUS data indicate significantly higher spectral content at high frequencies compared to WUS rock motion of comparable magnitudes and distances (Fletcher, 1995; Silva and Darragh, 1995).

APPENDIX C

2.1 Shallow Crustal Damping

The difference in spectral content can perhaps be most easily seen in spectral amplification (S_a/a) computed from recordings typical of WUS and CEUS tectonic environments. Figure C-1 shows average spectral shapes (S_a/a) computed from recordings made on rock at close distances (≤ 25 km) to M approximately $6\frac{3}{4}$ and $5\frac{1}{4}$ earthquakes in CEUS and WUS tectonic environments. The differences are significant and indicate that CEUS spectral content is higher than that in WUS for frequencies greater than approximately 10 Hz.

The controlling mechanism for the differences in high frequency spectral content (at close distances) between WUS and CEUS ground motions is thought to be due to differences in damping in the shallow (1 to 2 km) part of the crust (Boore and Atkinson, 1987; Silva et al., 1989a, 1989b; Silva, 1991; Silva and Darragh, 1995). The effects of shallow crustal damping were first pointed out and quantified by Hanks (1982) and Anderson and Hough (1984). The parameter which controls the shallow damping is termed κ and is defined as the thickness of the zone over which the damping is taking place times the damping and divided by the average velocity over zone of damping.

In a recent study, κ values were estimated by fitting spectral shapes computed from the stochastic ground motion model to shapes computed from motions recorded at rock sites in CENA, WUS, Mexico, Italy (Friuli), USSR (Gazli), and Taiwan (SMART1) (Silva and Darragh, 1995). Results of these analyses indicate that κ is strongly dependent upon the material properties of the site. Rock sites characterized as soft, such as sedimentary, showed significantly higher κ values than those characterized as hard, e.g. crystalline basement. Hard and soft rock sites may exist in

APPENDIX C

either WUS or CEUS; however, on the average, sites in stable cratonic regions are more likely to be classified as hard while those associated with active tectonic regions are more likely to be soft.

2.2 Crustal Amplification

An example of generic crustal models reflecting typical WUS soft rock and CEUS hard rock crustal conditions is shown in Figure C-2 for both compression- and shear-wave velocities. The CEUS model is the midcontinent structure from EPRI (1993) and is considered appropriate for strong ground motion propagation in central and eastern North America except for the Gulf Coast region (Toro et al., 1997). The Gulf Coast region is typified by a crustal structure somewhat intermediate between those of the CEUS and WUS and is predicted to have correspondingly different wave propagation characteristics and strong ground motions (EPRI, 1993; Toro et al., 1997). The WUS model reflects an average of several California crustal models (Silva et al., 1997) representing the most seismically active regions, the north coast and peninsular range areas. The shallow portion of the WUS crustal model (with $V_s \leq 1$ km/sec) is based on velocities measured at strong motion rock sites, such sites generally show very low near surface (0 to 30m) shear- and compression-wave velocities (Boore and Joyner 1997).

The differences in the shallow crustal velocities between the WUS and CEUS models is striking, particularly over the top 2 to 3 km, and the effects on strong ground motions are profound. In terms of amplification from source regions below about 5 km to the surface, the differences between hard (CEUS) and soft (WUS) crustal conditions results in a difference of a factor near 3 in amplification for frequencies exceeding about 5 Hz (Figure C-3). All else being equal, WUS high frequency ($f \geq 5$ Hz) ground motions would then be expected to be nearly three times larger than

APPENDIX C

corresponding CEUS motions. As suggested earlier however, pervasive observations reflect the converse, high frequency CEUS motions generally exceed comparable WUS motions. Damping in the shallow crust, parameterized through kappa, is much greater in soft crustal rocks resulting in a dramatic loss in high frequency energy content compared to hard rock conditions. The differences in shallow crustal damping, or kappa, between soft and hard crustal conditions is a combined effect of lower velocities (Figure C-2) as well as larger intrinsic damping. Kappa is defined as

$$\kappa = \frac{H}{\overline{V_s} \overline{Q_s}}, \quad \overline{Q_s} = \frac{1}{2 \overline{\eta_s}} \quad (\text{C-1})$$

where H is the thickness of the shallow crustal damping zone (1 to 2 km, Anderson and Hough, 1984; Silva and Darragh, 1995), $\overline{V_s}$ and $\overline{Q_s}$ are the average shear-wave velocities and quality factors over depth H, and $\overline{\eta_s}$ is the corresponding critical damping ratio (decimal). For soft rock conditions both the velocities and Q values are lower than hard rock conditions resulting in very large differences in kappa values and corresponding energy absorption at high frequency. Table C1 lists kappa values determined at both WUS and CEUS rock sites (Silva and Darragh, 1995) and shows the strong dependence upon surficial geology in terms of rock quality. Hard and soft conditions can exist in both WUS and CEUS and are reflected in distinct kappa values, increasing as the rock quality degrades. On average, kappa values for the WUS are about 5 times larger than the CEUS (0.037 sec and 0.008 sec, Table C1). It is important to emphasize that kappa values and shallow crustal amplification are strongly related. In going from hard rock to soft rock conditions, not only kappa values change but shallow crustal velocities change as well (Equation C-1). Soft rock conditions are reflected in higher kappa values and corresponding lower shear- and compressional-wave velocities. The lower velocities result in larger amplification, counteracting the effects of

APPENDIX C

increased damping resulting from larger kappa values.

To illustrate the effects of kappa on strong ground motions, Figures C-4 and C-5 show response spectral shapes (5% damping) and absolute spectra computed for an **M** 6.5 earthquake occurring at a distance of 25 km for WUS parameters (Table C2) using a range of kappa values from 0.005 sec to 0.160 sec. For the shapes, Figure C-4, increasing kappa results in a shift in shapes to lower frequencies as the peak accelerations (normalization parameters) and high frequency spectral amplitudes decrease. For fixed magnitude, the frequency range of maximum spectral amplification is a good estimator of shallow crustal damping (Silva and Darragh, 1995).

The absolute spectra shown in Figure C-5 further illustrate the effects of kappa on high frequency strong ground motions. A 100% change in kappa results in about a 50% change in peak acceleration. The average difference in WUS and CEUS rock site kappa values of about 5 (Table C1) results in a difference of about a factor of four in high frequency ground motions, exceeding the factor of about three in the difference in high frequency (5 Hz) crustal amplification (Figure C-3). Close-in strong ground motions (≤ 50 km), where differences in deep crustal properties such as frequency dependent damping ($Q(f)$) and depth to the Moho and Conrad discontinuities do not have large effects (EPRI, 1993), would be expected to be lower at CEUS rock sites than WUS rock sites at low frequencies. At high frequencies the converse would be expected, providing source processes are similar in both regions. Several lines of evidence suggest that this is not the case however, with CEUS sources being more energetic, particularly at high frequencies, than WUS sources for the same **M**.

APPENDIX C

2.3 Source Processes

Another issue of consideration regarding the differences in spectral composition between WUS and CEUS strong ground motions at rock sites is the probable differences in earthquake source processes. Prior to the occurrence of the 1998 **M** 5.8 Saguenay earthquake, there was thought to be a difference of about two in stress drop (the difference in stress across the rupture surface before and after an earthquake) between WUS and CEUS sources with the CEUS having larger values, about 100 bars compared to about 50 bars (Atkinson, 1989; Boore, 1986). These measures of stress drop, termed Brune stress drops (Brune, 1970; Appendix D), are primarily based on high frequency ground motion levels assuming a single-corner frequency source model.

An alternative measure of stress drop is based on the ratio of the seismic moment (M_o) to the rupture area and is termed the static stress drop. The stress drop equation for a circular rupture surface is given by

$$\Delta\sigma = \frac{7}{16} \pi \frac{M_o}{\left(\frac{A}{\pi}\right)^{\frac{4}{3}}}, \quad (\text{C-2})$$

where A is the rupture area. This measure of stress drop was also thought to be higher, by about a factor of two for earthquakes occurring in the CEUS compared to WUS (Kanamori and Anderson, 1975; Kanamori and Allen, 1986). For static stress drops, the scaling of strong ground motions is not at all clear. However, since the average slip (fault displacement) is proportional to moment and strong ground motions increase with slip (for fixed rupture area), strong ground motions, at least at low frequency, must increase with static stress drop.

APPENDIX C

Apart from the differences in stress drops (Brune and static), overall source processes were thought to be similar in both tectonic regimes. The stochastic single-corner-frequency point-source model (Appendix D), originally developed by Hanks and McGuire (1981), provides accurate predictions of WUS strong ground motions using a stress drop of about 50 bars (Boore, 1986; Boore et al., 1992; Silva and Darragh, 1995) although with a tendency to overpredict low frequency (≤ 1 Hz) motions for large magnitude earthquakes (Atkinson and Silva, 1997).

For the CEUS, the simple point-source model with a stress drop of about 100 bars, about double that of the WUS, provided good agreement with existing data (Atkinson, 1984; Boore and Atkinson, 1987; Toro and McGuire, 1987) until the occurrence of the 1988 **M** 5.8 Saguenay earthquake. Strong ground motions from this earthquake, the largest to have occurred in the CEUS in over 50 years, depart significantly from predictions of the simple 100 bar stress drop model (Boore and Atkinson, 1992). The stress drop required to match high frequency strong ground motions for this earthquake exceed 500 bars, while the intermediate frequency spectral levels are overestimated by a factor of two or more, requiring a significantly lower stress drop (Boore and Atkinson, 1992). Concurrently, Boatwright and Choy (1992) using teleseismic (low frequency, ≤ 2 Hz) data, showed that the source spectra of large intraplate earthquakes differ in general from the simple single-corner-frequency omega-square model, showing the presence of a second corner frequency. Based on the limited ground motion data in the CEUS as well as inferences on intensity observations, Atkinson (1993) developed an empirical two-corner source model for CEUS earthquakes. In this model, the high frequency spectral levels are consistent with Brune stress drop of about 150 bars while the equivalent stress drop for the low frequency spectral levels is about 40 to 50 bars (Atkinson, 1993), assuming the crustal model shown in Figure C-2. This two-corner model currently provides

APPENDIX C

unbiased estimates of recorded CEUS ground motions over the frequency range of the majority of the data, about 10.0 to 0.1 Hz, while the single-corner-frequency model, with stress drops ranging from about 120 to 150 bars, overpredicts low frequency ground motions in the frequency range of about 1 Hz to 0.1 Hz but is unbiased in the 2 to 10 Hz frequency range (Atkinson and Boore, 1998). Both the double and single corner source models, with actual or implied stress drops below 200 bars, underpredict the high frequency (≥ 2 Hz) ground motions for the Saguenay earthquake by factors of 2 to 3 suggesting anomalous high frequency levels for this event. While it currently appears that the two-corner source model may be the more appropriate model for CEUS strong ground motions, it is evident that in predicting strong ground motions for engineering design, significantly more variability should be accommodated in applications to the CEUS than to the WUS. This increased variability should accommodate both randomness (aleatory variability) in stress drop above that for the WUS as well as uncertainty (epistemic variability) in the source model.

For the WUS, recent work has shown some interesting results regarding earthquake source spectra. In the context of the single-corner-frequency model, stress drop appears to be magnitude dependent (Silva and Darragh, 1995; Atkinson and Silva, 1997; Silva et al., 1997), decreasing from about 100 bars for M 5.5 to about 50 bars for M 7.5 with an average value over magnitude of about 70 bars. Since inferences on stress drop for CEUS sources are based predominately on small magnitude earthquakes, $M \approx 5.2$ (Atkinson, 1993), scaling of stress drop with magnitude similar to WUS would imply significantly lower stress drops for large magnitude earthquakes. The 150 bar stress drop for CEUS may reflect a value appropriate for M near 5.5. Assuming WUS stress drop scaling with M would result in an average stress drop of about 120 bars for M ranging from 5.5 to 7.5.

APPENDIX C

A model which appears to be more consistent with WUS source spectra inferred from the strong motion data is similar to the CEUS two corner model but with a less pronounced spectral sag at intermediate frequencies. The two-corner nature of WUS source spectra is filled-in by crustal amplification (Figure C-3) resulting in a comparatively subtle feature in strong ground motions compared to CEUS data (Atkinson and Silva, 1997). This observation may provide some comforting linkage to CEUS source processes suggesting an appealing underlying similarity. However, CEUS sources, for the same magnitude, do appear to be considerably more energetic at high frequency which is reflected in larger Brune stress drops by a factor of about two on average.

To illustrate the effects of stress drop on ground motions, Figures C-6 and C-7 show response spectral shapes (5% damping) and absolute spectra computed for $M 6.5$ at a distance of 25 km using WUS parameters (Table C2). For the shapes, Figure C-6, the effect of stress drop is small, with differences occurring at low frequency below about 1 Hz. Spectral shapes are largely independent of stress drop for ranges of 2 to 3 over most of the frequency band of interest.

The absolute spectra shown in Figure C-7 illustrate the large effect Brune stress drops have on strong ground motions. The effect is strongest for frequencies exceeding the source corner frequency (Silva, 1993), about 0.2 Hz for a stress drop of 65 bars, and results in about a 70% change in peak acceleration for a 100% change in stress drop. For the single-corner-frequency Brune source model, stress drop is a controlling parameter in absolute levels of strong ground motions.

Comparisons of WUS to CEUS response spectra are shown in Figures C-8 and C-9 for shapes and absolute spectra respectively. Also illustrated in the Figures are the differences between

APPENDIX C

the single and double corner source spectral models. For the shapes, Figure C-8, the difference in spectral composition between the WUS and CEUS single corner models (solid lines) is clearly illustrated in the maximum spectral amplifications: about 5 Hz for WUS and 40 Hz for CEUS.

The difference between the single and double corner source models (solid versus dashed lines) is also clearly illustrated. For the WUS, the difference is mainly at low frequency and is not large, about 20% near 0.3 Hz. For the CEUS, the single corner source model significantly exceeds the double corner below about 2 Hz. The largest difference occurs near 0.4 Hz and is a factor of over 3 in 5% damped spectral acceleration. Choices between the two shapes for the CEUS, single or double corner, clearly have major impacts on design motions.

The corresponding absolute spectra (not scaled) are shown in Figure C-9. The WUS and CEUS single corner spectral estimates are nearly the same for frequencies up to about 5 Hz. This is the result of compensating effects previously discussed, higher stress drop for CEUS (Table C2) and larger amplification factors for WUS (Figure C-3). Beyond about 5 Hz, the differences in kappa values (0.04 sec compared to 0.006 sec, Table C2) results in the differences in high frequency spectral estimates.

To see how well the simple point-source models (single and double corner frequency) capture the differences in shapes between WUS and CEUS rock motions which were illustrated in Figure C-1, Figures C-10 and C-11 compare model predictions to $M^{6\frac{3}{4}}$ statistical shapes. Figure C-10 for WUS, compares both the single and double corner model predictions to the statistical shape. Both models capture the overall shape reasonably well but overpredict at low frequency (below 1 to 2 Hz). The double corner model provides a better fit but still shows overprediction in this magnitude range.

APPENDIX C

The comparison to CEUS $M 6.8$ is shown in Figure C-11. There is only one earthquake 1985 Nahanni, with hard rock site recordings (3 stations) in this distance range. Both spectral models capture the difference in shape between WUS and CEUS equally well with the single corner frequency model showing an overprediction at low frequency (≤ 1 Hz) similar to the WUS. Interestingly, the double corner model shows an underprediction for frequencies below about 2 Hz. Since this is only a single earthquake and variability is large in CEUS strong ground motions, these results should not be interpreted as a potential bias in the model for spectral shapes but do emphasize the current state of uncertainty regarding CEUS strong ground motions.

For the $M 5\frac{3}{4}$ comparison, Figures C-12 and C-13 show results for WUS and CEUS respectively. For the WUS, Figure C-12 shows reasonable model predictions down to about 1 Hz, below which the number of spectra are rapidly dropping out due to increasing noise levels. Figure C-13 shows the corresponding plot for CEUS $M 5\frac{3}{4}$ comparisons. The models capture the shift in shape to higher frequency but overpredict for frequencies above about 20 Hz. As with the $M 6\frac{3}{4}$ comparison, the low frequencies are enveloped by the two models. Since the $M 5\frac{3}{4}$ statistical shape reflects the same Nahanni earthquake sequence, average of only 2 aftershocks, model departures, although discomfoting, are not considered particularly significant.

These comparison to CEUS statistical shapes point out the quandary in estimating strong ground motions in the CEUS. Sufficient recordings at close distances (≤ 50 km) for earthquakes of engineering significance ($M \geq 5$) are not available to unequivocally distinguish between plausible models.

APPENDIX C

REFERENCES

- Anderson, J. G. and S. E. Hough (1984). "A Model for the Shape of the Fourier Amplitude Spectrum of Acceleration at High Frequencies." *Bulletin of the Seismological Society of America*, 74(5), 1969-1993.
- Atkinson, G.M. and Boore, D.M. (1998). "Evaluation of models for earthquake source spectra in Eastern North America." *Bull. Seism. Soc. Am.* 88(4), 917-934.
- Atkinson, G.M. and S.Z. Chen (1997). "Regional seismograms from historical earthquakes in southeastern Canada." *Seism. Res. Lett.* 68(5), 797-807.
- Atkinson, G.M. and W.J. Silva (1997). "An empirical study of earthquake source spectra for California earthquakes." *Bull. Seism. Soc. Am.* 87(1), 97-113.
- Atkinson, G.M. (1996). "The high-frequency shape of the source spectrum for earthquakes in eastern and western Canada." *Bull. Seism. Soc. Am.* 86(1A), 106-112.
- Atkinson, G.M. and D.M. Boore (1995). "Ground motion relations for eastern North America." *Bull. Seism. Soc. Am.*, 85(1), 17-30.
- Atkinson, G.M. (1993). "Source spectra for earthquakes in eastern North America." *Bull. Seism. Soc. Am.*, 83(6), 1778-1798.
- Atkinson, G.M. (1984). "Attenuation of strong ground motion in Canada from a random vibrations approach." *Bull. Seism. Soc. Am.*, 74(5), 2629-2653.
- Benz, H.M., A. Frankel, and D.M. Boore (1997). "Regional L_g attenuation for the continental United States." *Bull. Seism. Soc. of Am.*, 87(3), 606-619.
- Boatwright, J. and G. Choy (1992). "Acceleration source spectra anticipated for large earthquakes in Northeastern North America." *Bull. Seism. Soc. Am.*, 82, 660-682.
- Boore, D.M, and W.B. Joyner (1997). "Site amplifications for generic rock sites." *Bull. Seis. Soc. Am.*, 87(2), 327-341.
- Boore, D.M. and G.M. Atkinson (1992). "Source spectra for the 1988 Saguenay, Quebec, earthquakes." *Bull. Seism. Soc. Am.*, 82(2), 683-719.
- Boore, D.M., W.B. Joyner, and L. Wennerberg (1992). "Fitting the stochastic ω^{-2} source model to observed response spectra in western North America: Trade-offs between $\Delta\sigma$ and κ " *Bull. Seism. Soc. Am.*, 82(4), 1956-1963.

APPENDIX C

Boore, D.M. and G.M. Atkinson (1987). "Stochastic prediction of ground motion and spectral response parameters at hard-rock sites in eastern North America." *Bull. Seism. Soc. Am.*, 77(2), 440-467.

Boore, D.M. (1986). "Short-period P- and S-wave radiation from large earthquakes: implications for spectral scaling relations." *Bull. Seism. Soc. Am.*, 76(1) 43-64.

Borcherdt, R. D. (1986). "Preliminary Report on Aftershock Sequence for Earthquake of January 31, 1986 near Painesville, Ohio." U.S. Geological Survey Open File Report 86-181.

Brady, A.G., P.N. Mork, and J.P. Fletcher (1981). "Processed accelerograms from Monticello Dam, Jenkinsville, South Carolina, August 27, 1978, and two later shocks." *USGS Open-File Rept.* 81-448.

Brune, J.N. (1970). "Tectonic stress and the spectra of seismic shear waves from earthquakes." *J. Geophys. Res.* 75, 4997-5009.

Campbell, K.W. (1986). "An empirical estimate of near-source ground motion for a major ($m_b = 6.8$) earthquake in the Eastern United States." *Bull. Seism. Soc. Am.*, 76, 1-17.

Campbell, K. W. (1981). "A Ground Motion Model for the Central United States Based on Near-Source Acceleration Data." In *Proc. of Conf. on Earthquakes and Earthquake Engineering: the Eastern United States.*, edited by J. E. Beavers, Knoxville, Tennessee, September 14-16, Ann Arbor Science Publishers, 1, 213-222.

Chang, F.K. (1983). "Analysis of strong motion data from the New Hampshire earthquake of 18 January 1982,." US Nuclear Regulatory Commission Rept. NUREG/CR-3327.

Cranswick, E., R., Wetmiller, and J. Boatwright (1985). "High-frequency observations and source parameters of microearthquakes recorded at hard-rock sites." *Bull. Seism. Soc. Am.*, 75(6), 1535-1567.

Electric Power Research Institute (1993). "Guidelines for determining design basis ground motions." Palo Alto, Calif: Electric Power Research Institute, vol. 1-5, EPRI TR-102293.

vol. 1: Methodology and guidelines for estimating earthquake ground motion in eastern North America.

vol. 2: Appendices for ground motion estimation.

vol. 3: Appendices for field investigations.

vol. 4: Appendices for laboratory investigations.

vol. 5: Quantification of seismic source effects.

Frankel, A. (1994). "Implications of felt area-magnitude relations for earthquake scaling and the average frequency of perceptible ground motion." *Bull. Seism. Soc. Am.*, 84(2), 462-465.

Frankel, A., A. McGarr, J. Bicknell, J. Mori, L. Seeber, and E. Cranswick (1990). "Attenuation of

APPENDIX C

high-frequency shear waves in the crust: Measurements from New York State, South Africa, and southern California." *J. Geo. Research*, 95(B11), 17,441-17,457.

Fletcher, J.B., (1995). "Source parameters and crustal Q for four earthquakes in South Carolina." *Seismol. Research Lett.*, 66(4), 44-58.

Haar, L. C., J. B. Fletcher, and C. S. Mueller (1984). "The 1982 Enola, Arkansas Swarm and Scaling of Ground Motion in the Eastern United States." *Bull. Seism. Soc. Am.*, 74(6), 2463-2482.

Hanks, T.C. and A.C. Johnston (1992). "Common features of the excitation and propagation of strong ground motion for north American earthquakes." *Bull. Seism. Soc. Am.*, 82(1), 1-23.

Hanks, T.C. (1982). " f_{\max} ." *Bull. Seism. Soc. Am.*, 72(6), 1867-1879.

Hanks, T.C., and McGuire, R.K. (1981). "The character of high-frequency strong ground motion." *Bull. Seism. Soc. Am.*, 71(6), 2071-2095.

Herrmann, R.B. and O.W. Nuttli (1982). "Magnitude: the relation of M_L to $m_{bl.g.}$." *Bull. Seism. Soc. Am.*, 72(2), 389-397.

Kanamori, H., and Allen, C.R. (1986). "Earthquake repeat time and average stress drop." *Earthquake Source Mech., Am. Geophys. Union Geophys. Monogr.*, S. Das, J. Boatwright, C.H. Scholz, ed., 37, 227-235.

Kanamori, H., D.L. Anderson (1975). "Theoretical basis of some empirical relations in seismology." *Bull. Seismol. Soc. Am.*, 65, 1073-1095.

Kimball, J.K. (1983). "The use of site dependent spectra." *Proc. Workshop on Site-Specific Effects of Soil and Rock on Ground Motion and the Importance for Earthquake-Resistant Design*, Santa Fe, New Mexico, USGS Open-File Rept. 83-845, 410-422.

Mork, P. and A. G. Brady (1981). "Processed Accelerograms from Monticello Dam, Jenkinsville, South Carolina, October 16, 1979, 0706 UTC." *U.S. Geological Survey Open-File Report 81-1214*.

Munro, P. S. and D. Weichert. (1989). "The Saguenay earthquake of November 25, 1988: Processed strong motion records." *Geological Survey of Canada Open File/Dossier Public 1996*.

Nuttli, O. W. (1981). "Similarities and Differences between Western and Eastern United States Earthquakes, and their Consequences for Earthquake Engineering." In *Proceedings of the Conference on Earthquakes and Earthquake Engineering: the Eastern United States*, edited by J. E. Beavers, vol. 1, Ann Arbor Science Publishers, Inc., Ann Arbor, Michigan, 25-27.

Silva, W.J., N. Abrahamson, G. Toro, C. Costantino (1997). "Description and validation of the stochastic ground motion model." Submitted to Brookhaven National Laboratory, Associated Universities, Inc. Upton, New York.

APPENDIX C

Silva, W.J. and R. Darragh (1995). "Engineering characterization of earthquake strong ground motion recorded at rock sites." Palo Alto, Calif:Electric Power Research Institute, TR-102261.

Silva, W.J. (1993). "Factors controlling strong ground motions and their associated uncertainties." *Seismic and Dynamic Analysis and Design Considerations for High Level Nuclear Waste Repositories*, ASCE 132-161.

Silva, W.J. (1991). "Global characteristics and site geometry." Chapter 6 in *Proceedings: NSF/EPRI Workshop on Dynamic Soil Properties and Site Characterization*. Palo Alto, Calif.: Electric Power Research Institute, NP-7337.

Silva, W.J., R. Darragh, R. Green, and F. Turcotte (1989a). "Spectral characteristics of small magnitude earthquakes with application to western and eastern North American tectonic environments: Surface motions and depth effects." U.S. Army Engineers Waterways Experiment Station Miscellaneous Paper G1-89-16.

Silva, W.J., R. Darragh, R. Green, and F. Turcotte (1989b). "*Estimated ground motions for a New Madrid event*." U.S. Army Engineers Waterways Experiment Station Miscellaneous Paper GL-89-17.

Singh, S. and R.B. Hermann (1983). "Regionalization of crustal coda Q in the continental United States." *J. Geophys. Res.*, 88, 527-538.

Toro, G.R., N.A. Abrahamson, and J.F. Schneider (1997). "Model of strong ground motions from earthquakes in Central and Eastern North America: Best estimates and uncertainties." *Seismological Research Let.*, 68(1), 41-57.

Toro, G.R. and R.K. McGuire (1987). "An investigation into earthquake ground motion characteristics in eastern North America." *Bull. Seism. Soc. Am.*, 77(2), 468-489.

Weichert, D. H., R. J. Wetmiller, R. B. Horner, P. S. Munro, and P. N. Mork (1986). "Strong Motion Records from the 23 December 1985, M_s 6.9 Nahanni, NWT, and Some Associated Earthquakes." *Geological Survey of Canada*, Open-File Report 1330.

Weichert, D. H., P. W. Pomeroy, P. S. Munro, and P. N. Mork (1982). "Strong motion records from Miramichi, New Brunswick, 1982 aftershocks." *Earth Physics Branch*, Ottawa, Canada, Open File Report 82-31.

Wesson, R. L. and C. Nicholson (1986). *Studies of the January 31, 1986 Northeastern Ohio Earthquake*. Report submitted to the U.S. Nuclear Regulatory Commission, U.S Geological Survey Open-File Report 86-331.

APPENDIX C

Table C1					
KAPPA VALUES FOR "AVERAGE" SITE CONDITIONS IN WUS AND CEUS*					
Tectonic	"Average" Site Condition	N	Median Kappa (sec)	σ_{in}	Range of Kappa for This Site Condition (sec)
WUS	Hard rock	11	0.026	0.58	0.010 - 0.060
	Weathered hard rock	9	0.035	0.52	0.015 - 0.100
	Soft rock	15	0.045	0.51	0.015 - 0.080
	Sheared rock	4	0.062	0.41	0.040 - 0.120
	Combined	39	0.037	0.59	0.010 - 0.120
CEUS	Hard rock	16	0.007	0.42	0.004 - 0.016
	Soft rock	3	0.017	0.09	0.015 - 0.018
	Sheared rock	1	0.025		0.025
	Combined	20	0.008	0.55	0.004 - 0.025

"Average" Site Condition is defined as:

Hard Rock: WNA as granite, schist, carbonate, slate
 ENA as granitic pluton, carbonate, sites in Canadian Shield region (Saguenay, New Hampshire).

Weathered hard rock: WNA as weathered granitic rock and tonalite

Soft rock: WNA as sandstone and breccias
 ENA as sandstone and claystone

Sheared rock: WNA as site near fault zone (Gilroy #6) or greenstone site in Franciscan (Redwood City, Hayward).
 ENA as site near fault zone (Nahanni River Site #1)

*Based on template fits to response spectral shapes (Silva and Darragh, 1995)

APPENDIX C

Table C2		
POINT-SOURCE PARAMETERS*		
	WUS	CEUS
$\Delta\sigma$ (bars)	65	120
kappa (sec)	0.040	0.006
Q_0	220	351
η	0.60	0.84
β (km/sec)	3.50	3.52
ρ (g/cc)	2.70	2.60
Amplification	soft rock (Figure C-2)	hard rock (Figure C-2)
Double Corner	Atkinson and Silva (1997)	Atkinson (1993)

*Parameters from Silva et al. (1997)

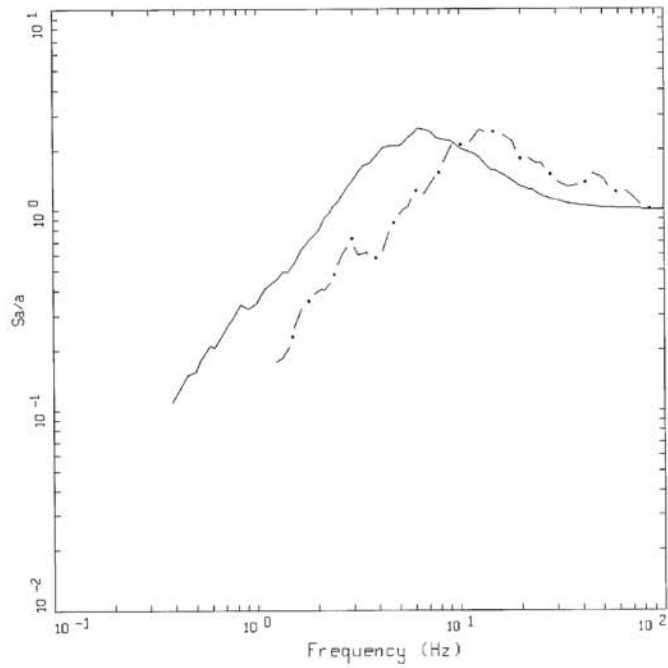
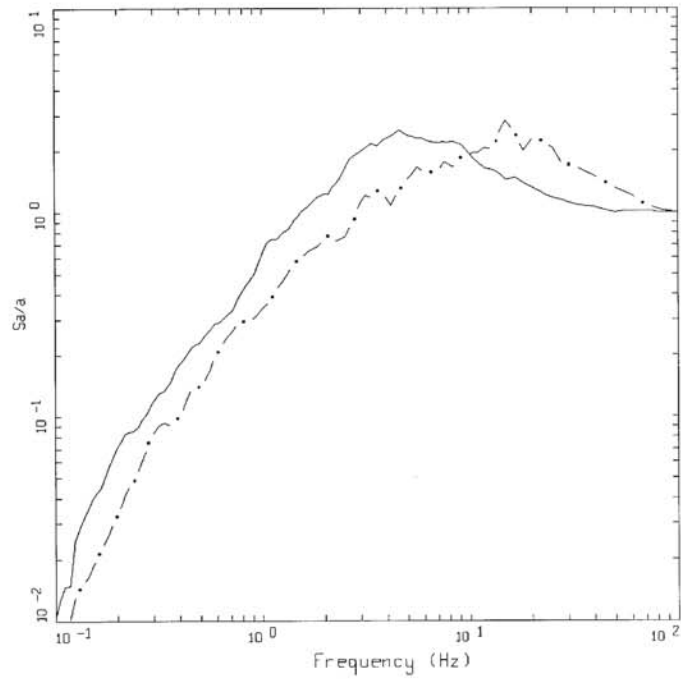
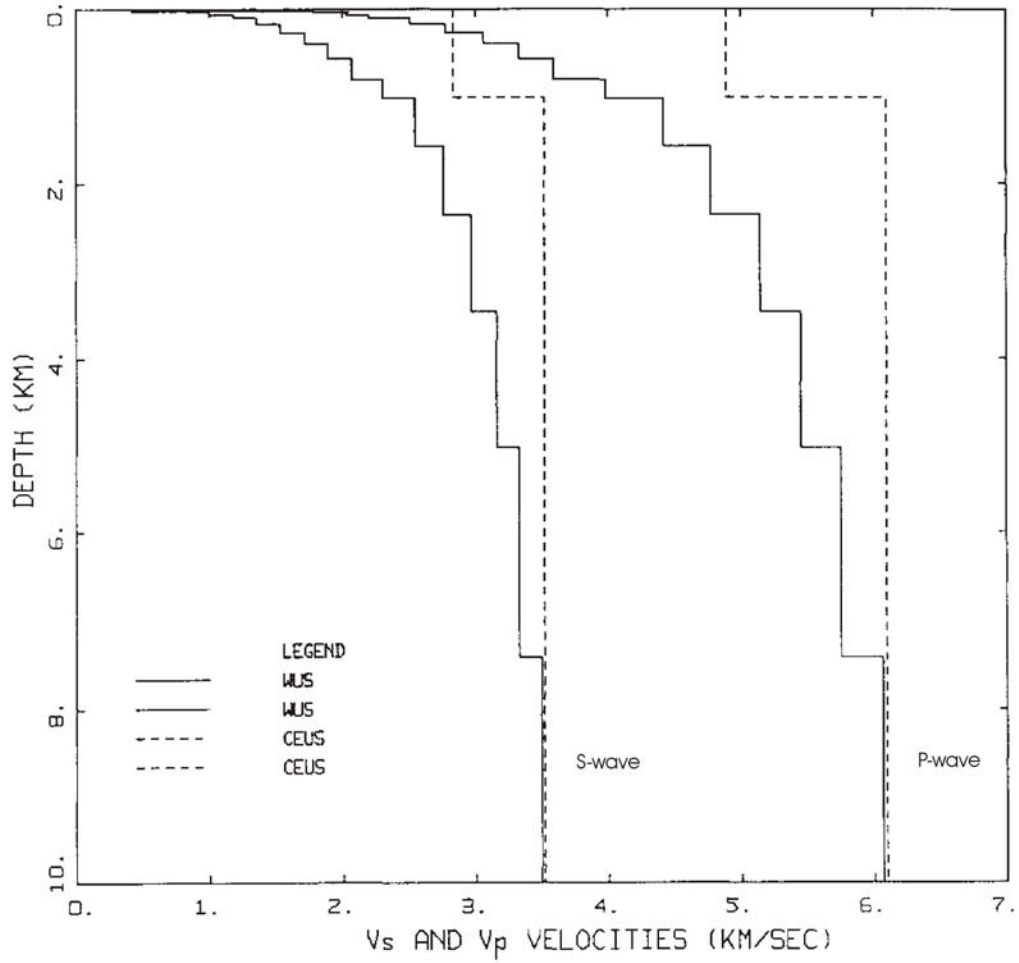
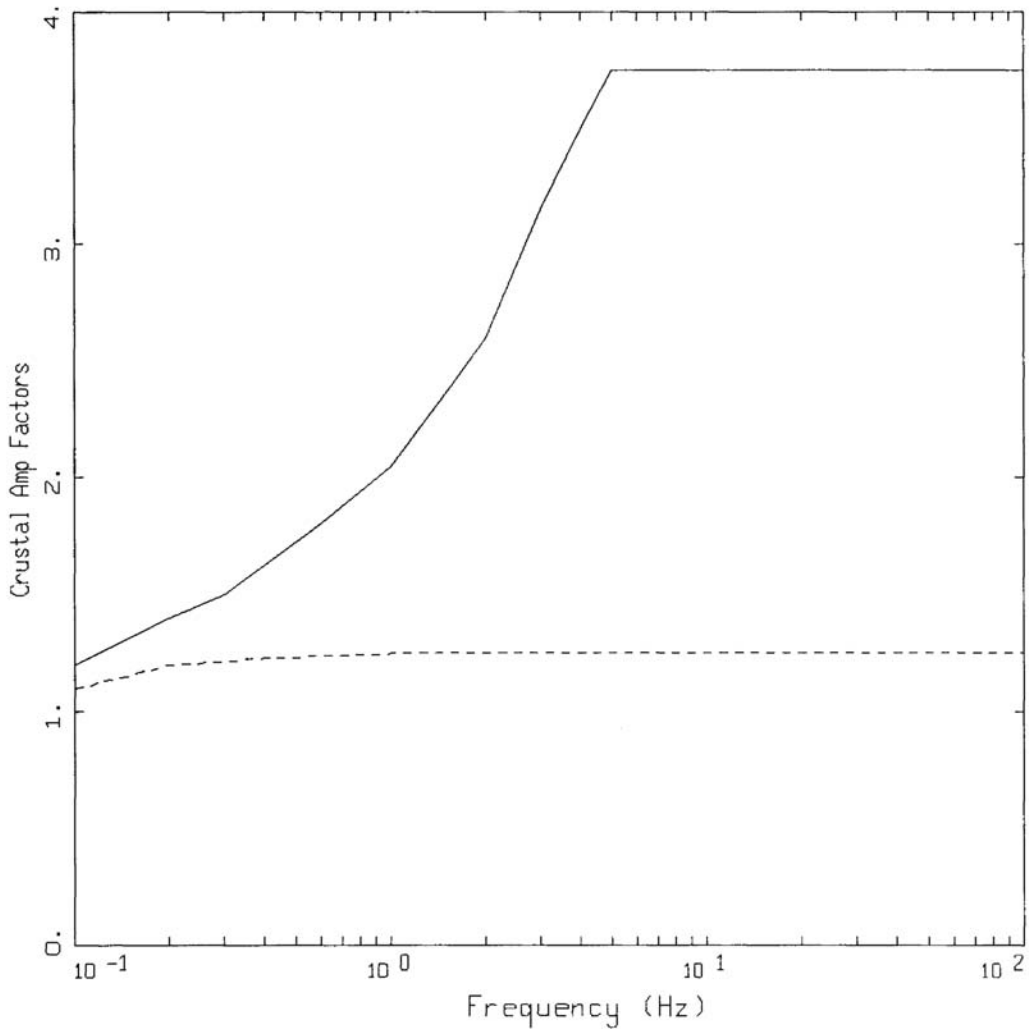


Figure C-1. Comparison of response spectral shapes (S_a/a_{max} , 5% damping) between CEUS (solid line), and WUS (dashed line) crustal conditions for earthquakes recorded at rock sites: $M 6\frac{3}{4}$ (upper) and $M 5\frac{3}{4}$ (lower).



GENERIC WUS AND CEUS
CRUSTAL MODELS

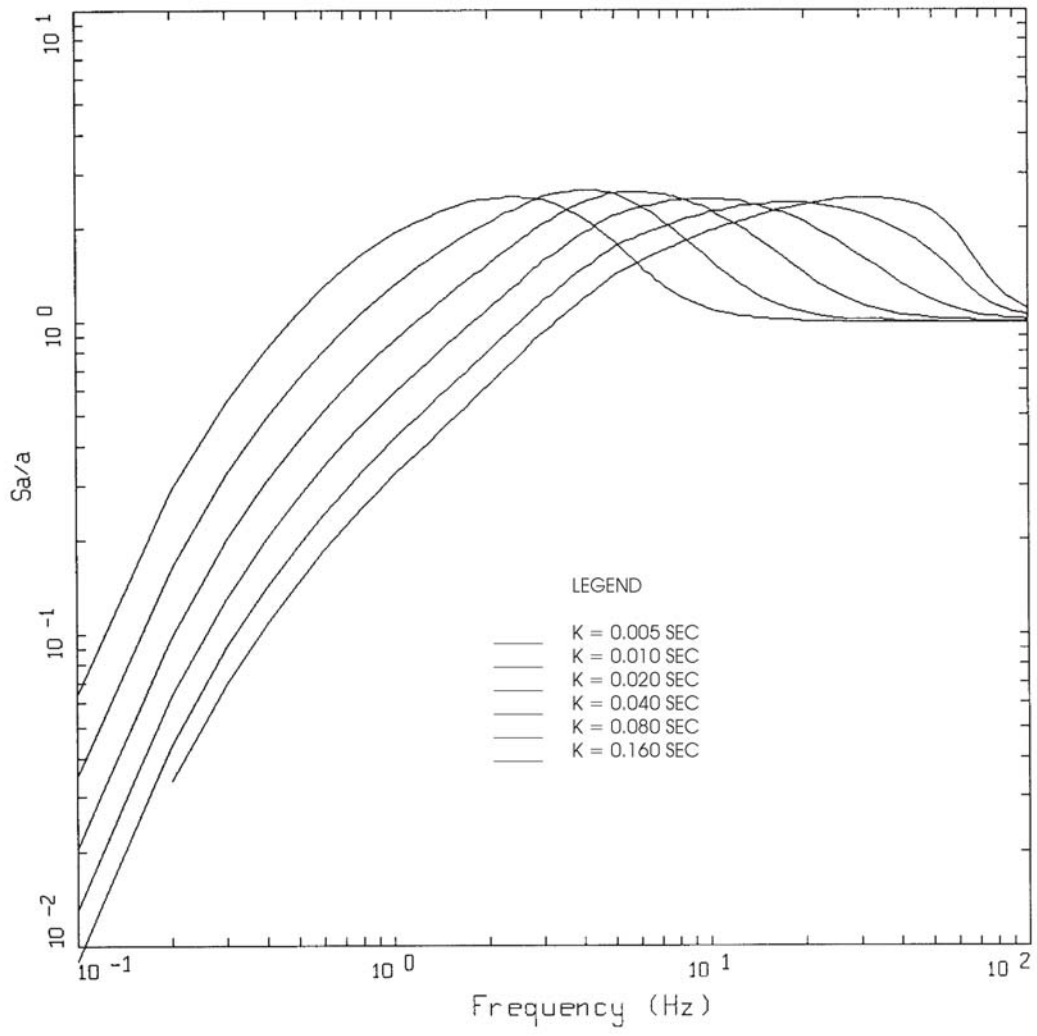
Figure C-2. Comparison of generic compression- and shear-wave velocity profiles for WUS (Silva et al., 1997) and CEUS (EPRI, 1993) crustal conditions.



CRUSTAL AMPLIFICATION FACTORS

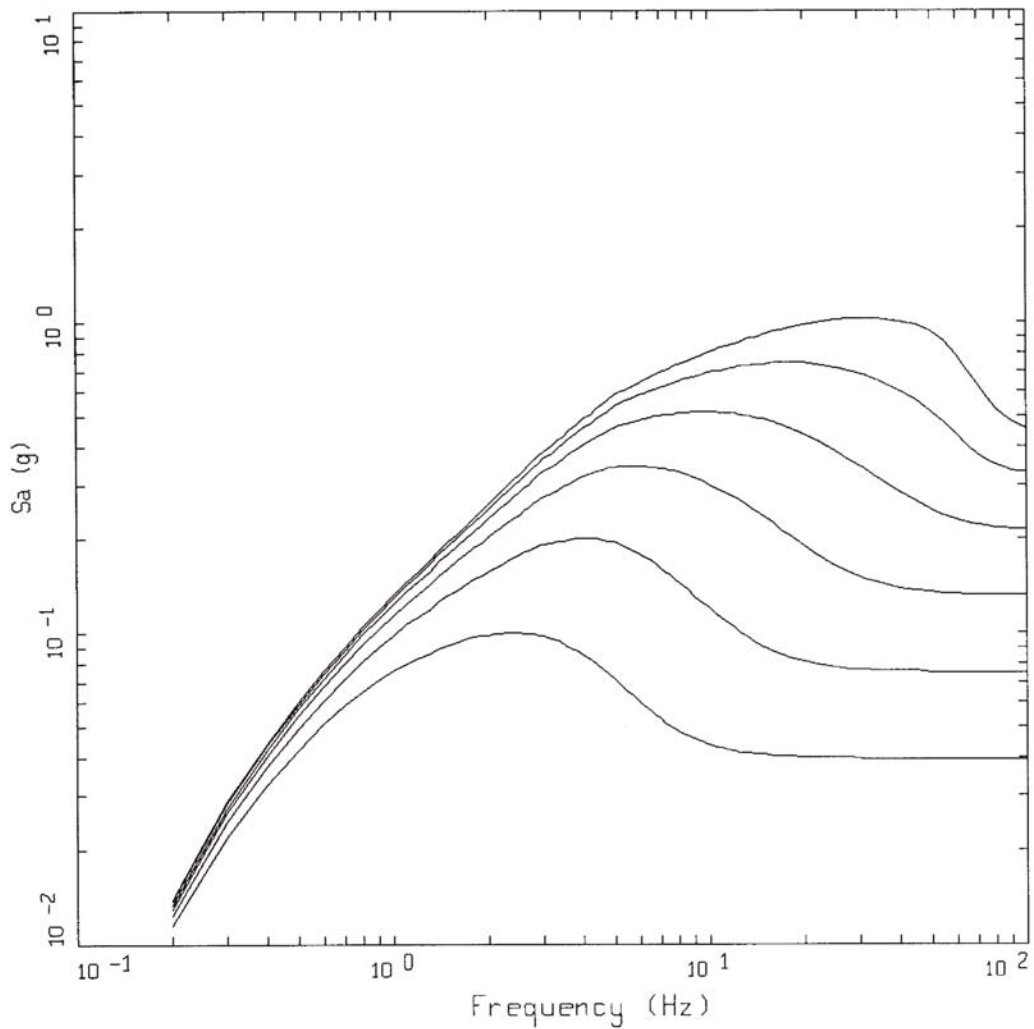
- LEGEND
- WUS, SOFT ROCK
 - - - CEUS, HARD ROCK

Figure C-3. Crustal amplification factors (smoothed) for Fourier amplitude spectra computed for the crustal models shown in Figure C-2 (10 km to the surface using vertically propagating shear-wave).



ROCK
 BASE CASE, WUS, 1-CORNER SOURCE MODEL
 M = 6.5, D = 25 KM, STRESS DROP = 65 BARS

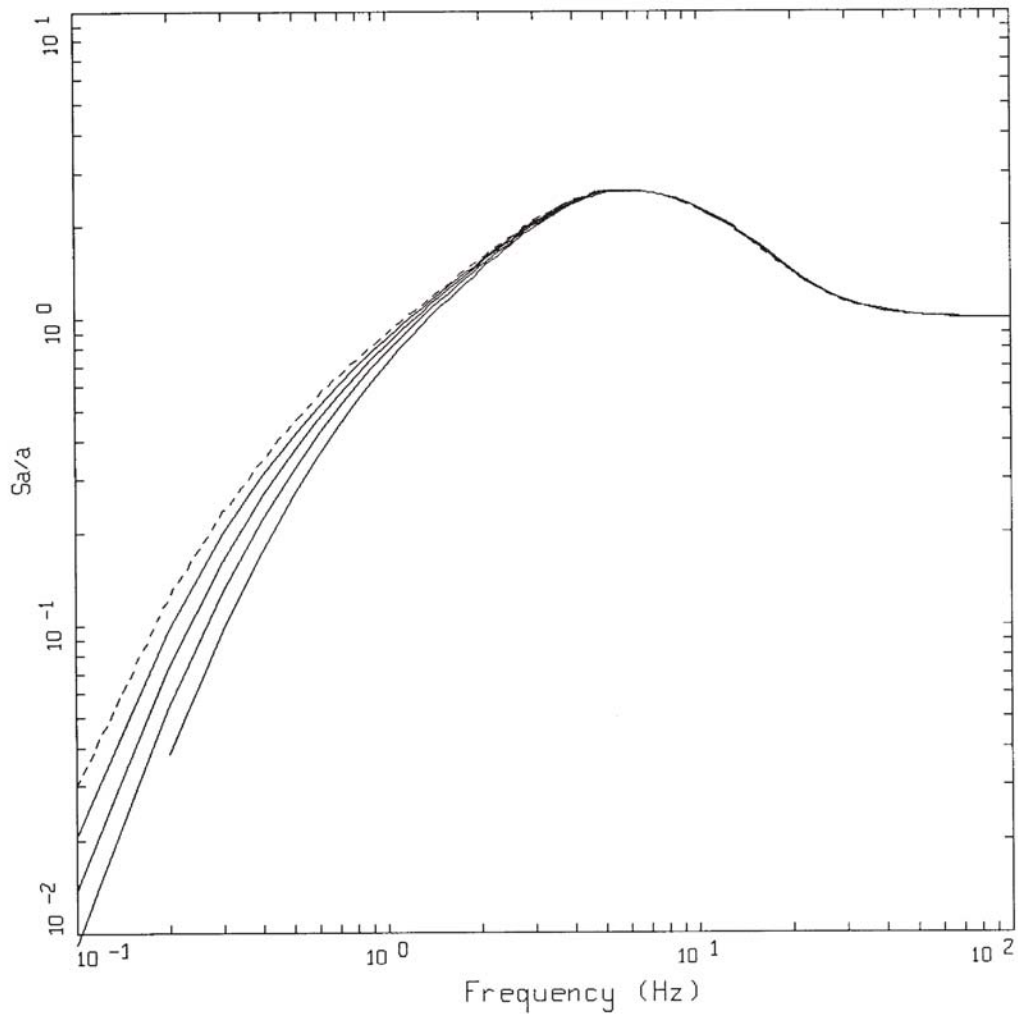
Figure C-4. Response spectral shapes (S_a/a_{max} , 5% damping) computed for **M** 6.5 at a distance of 25 km for a suite of kappa values using WUS parameters (Table C2).



ROCK
 BASE CASE, WUS, 1-CORNER SOURCE MODEL
 M = 6.5, D = 25 KM, STRESS DROP = 65 BARS

LEGEND	
—	K = 0.005 SEC
—	K = 0.010 SEC
—	K = 0.020 SEC
—	K = 0.040 SEC
—	K = 0.080 SEC
—	K = 0.160 SEC

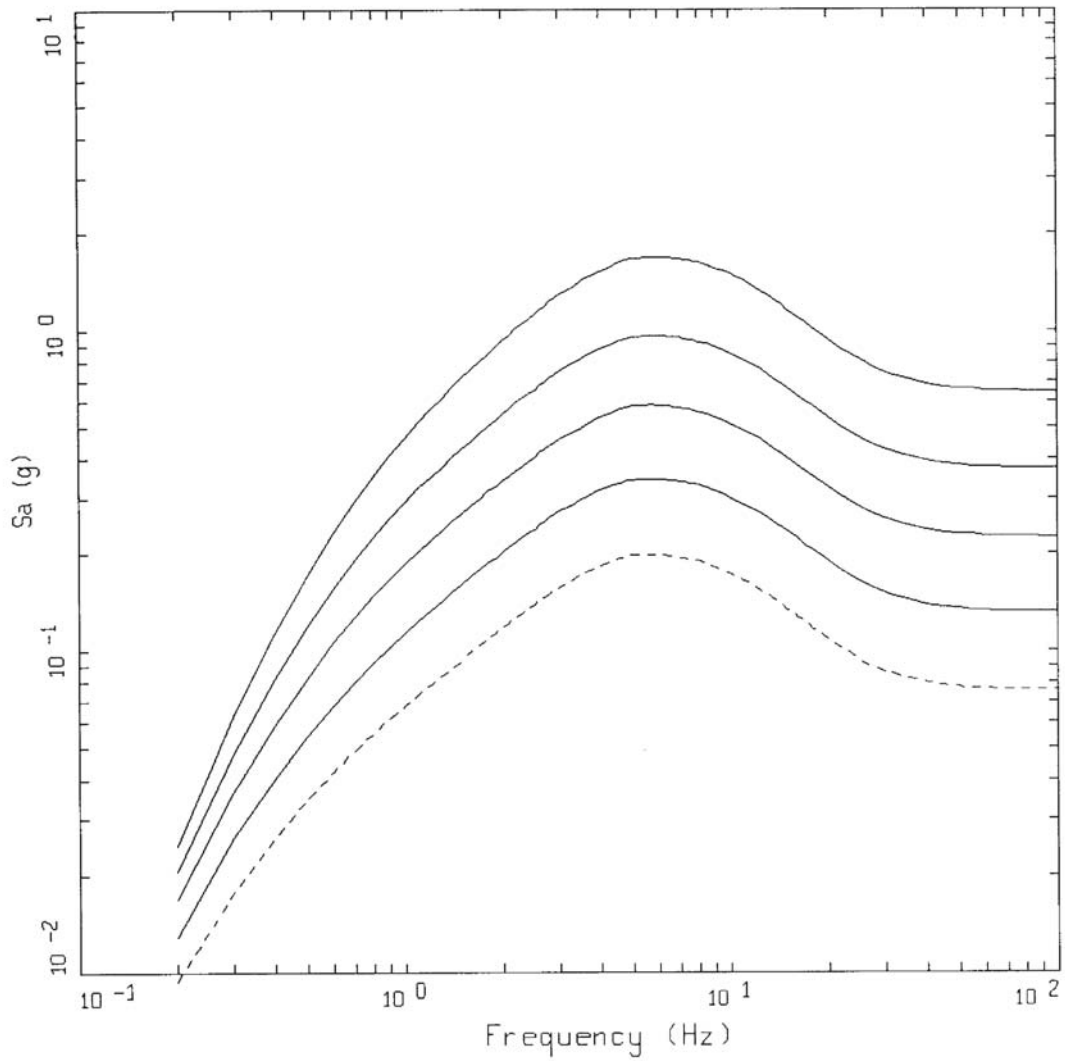
Figure C-5. Response spectra (5% damping) computed for an **M** 6.5 earthquake at a distance of 25 km for a suite of kappa values using WUS parameters (Table C3).



ROCK
 BASE CASE, WUS, 1-CORNER SOURCE MODEL
 M = 6.5, D = 25 KM, KAPPA = 0.040 SEC

- LEGEND
- STRESS DROP = 32 BARS
 - STRESS DROP = 65 BARS
 - STRESS DROP = 130 BARS
 - STRESS DROP = 260 BARS
 - STRESS DROP = 520 BARS

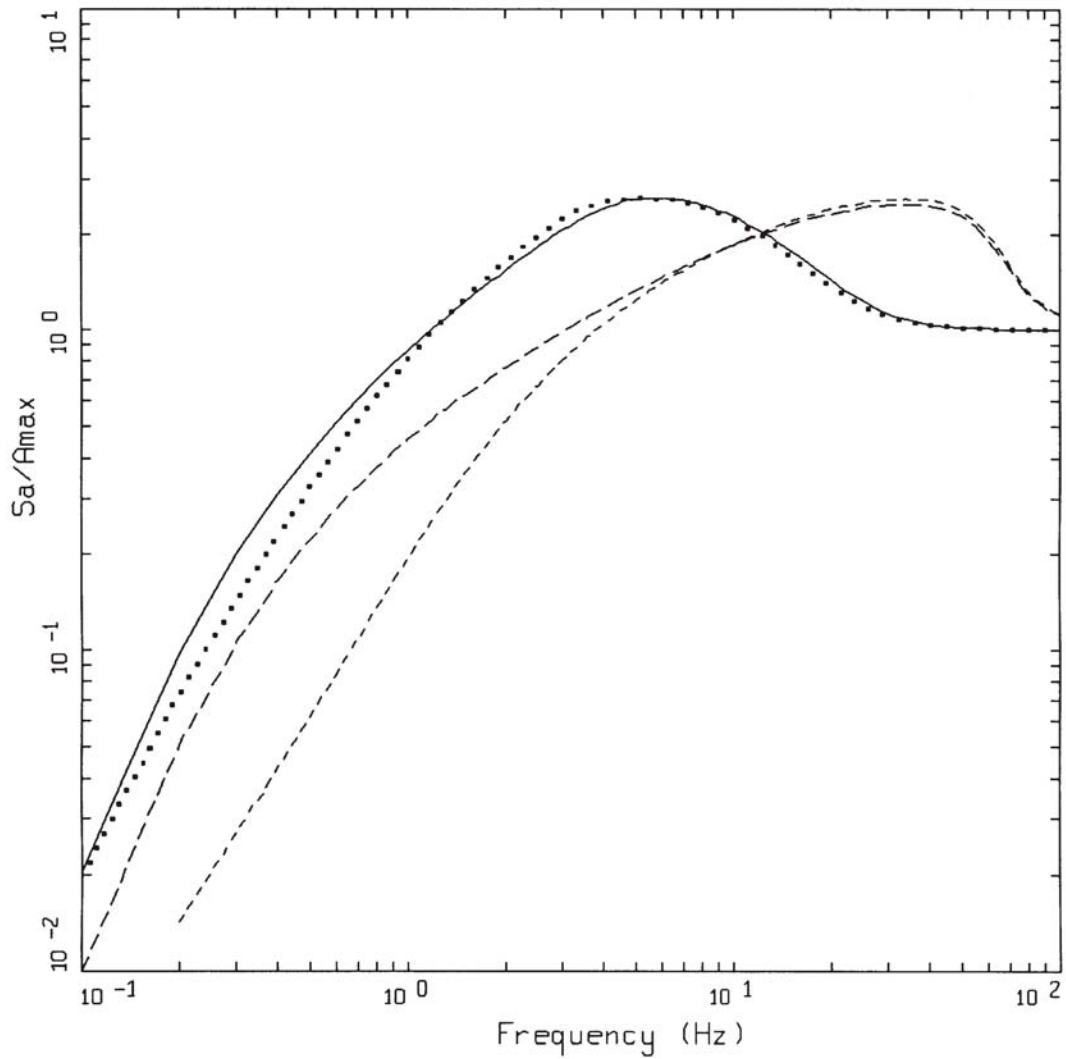
Figure C-6. Response spectral shapes (S_a/a_{max} , 5% damping) computed for M 6.5 at a distance of 25 km for a suite of stress drop values using WUS parameters (Table C2).



ROCK
 BASE CASE, WUS, 1-CORNER SOURCE MODEL
 M = 6.5, D = 25 KM, KAPPA = 0.040 SEC

- LEGEND
- STRESS DROP = 32 BARS
 - STRESS DROP = 65 BARS
 - STRESS DROP = 130 BARS
 - STRESS DROP = 260 BARS
 - STRESS DROP = 520 BARS

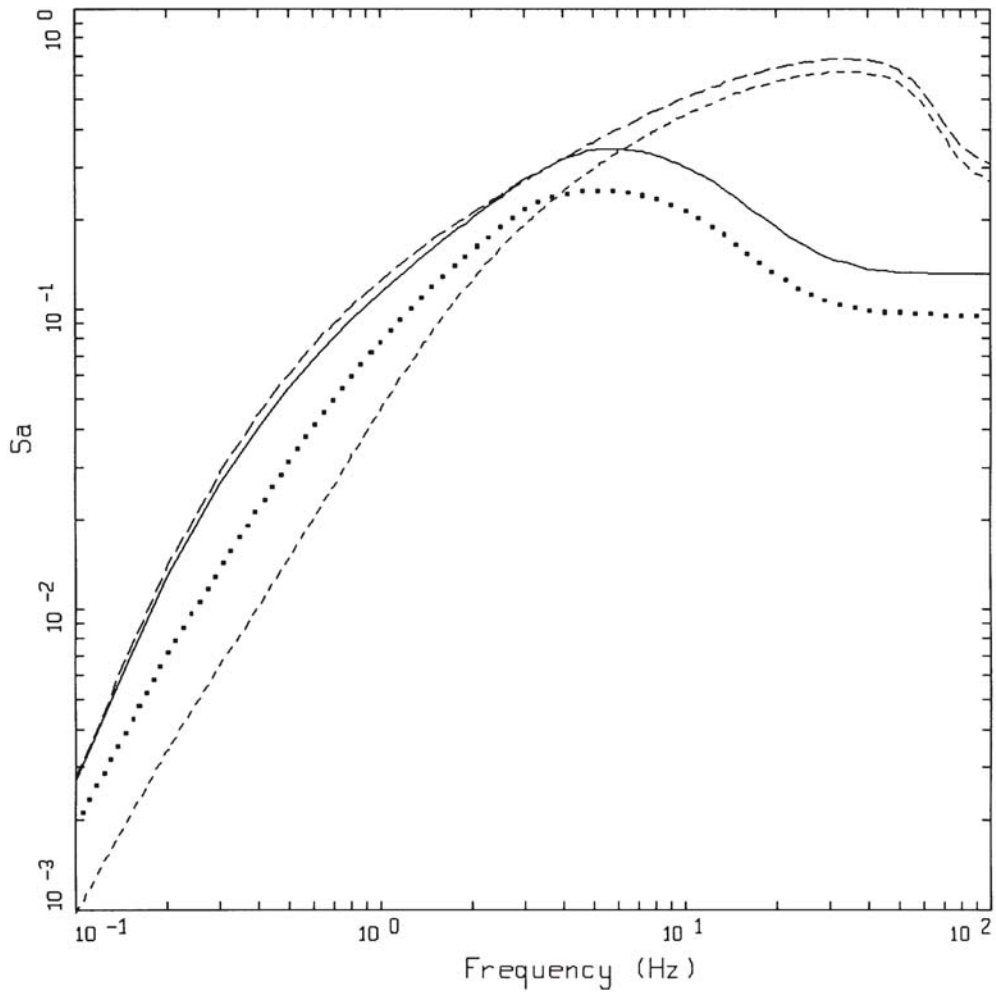
Figure C-7. Response spectra (5% damping) computed for M 6.5 at a distance of 25 km for a suite of stress drop values using WUS parameters (Table C2).



POINT-SOURCE MODEL
 $M = 6.5$, $R = 25$ KM

- LEGEND
- WUS ROCK, SINGLE CORNER
 - WUS ROCK, DOUBLE CORNER
 - - - CEUS ROCK, SINGLE CORNER
 - - - CEUS ROCK, DOUBLE CORNER

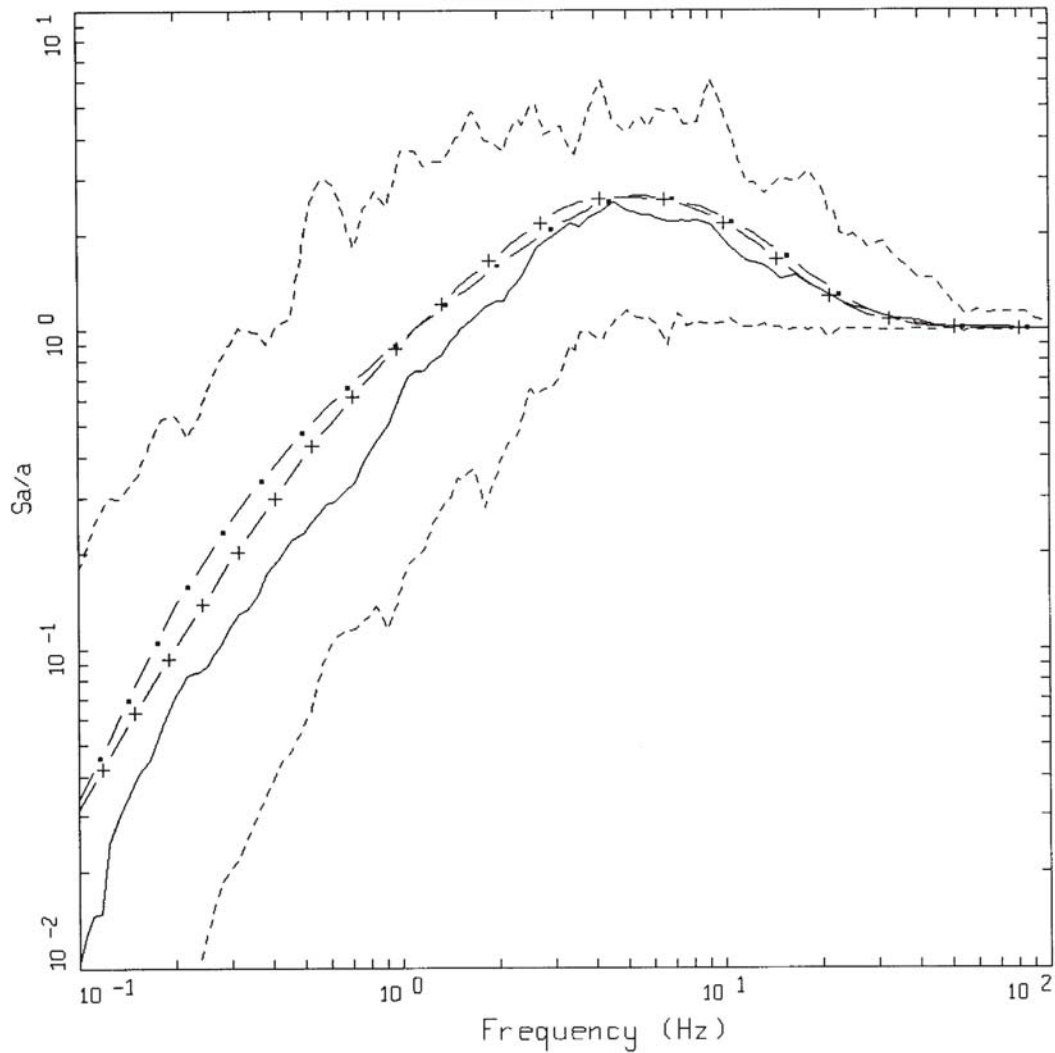
Figure C-8. Response spectral shapes (5% damping) computed for $M = 6.5$ at $R = 25$ km using both single and double corner frequency source spectra for WUS and CEUS conditions (Table C2).



POINT-SOURCE MODEL
 $M = 6.5$, $R = 25$ KM

- LEGEND
- WUS ROCK, SINGLE CORNER
 - WUS ROCK, DOUBLE CORNER
 - - - - CEUS ROCK, SINGLE CORNER
 - - - - CEUS ROCK, DOUBLE CORNER

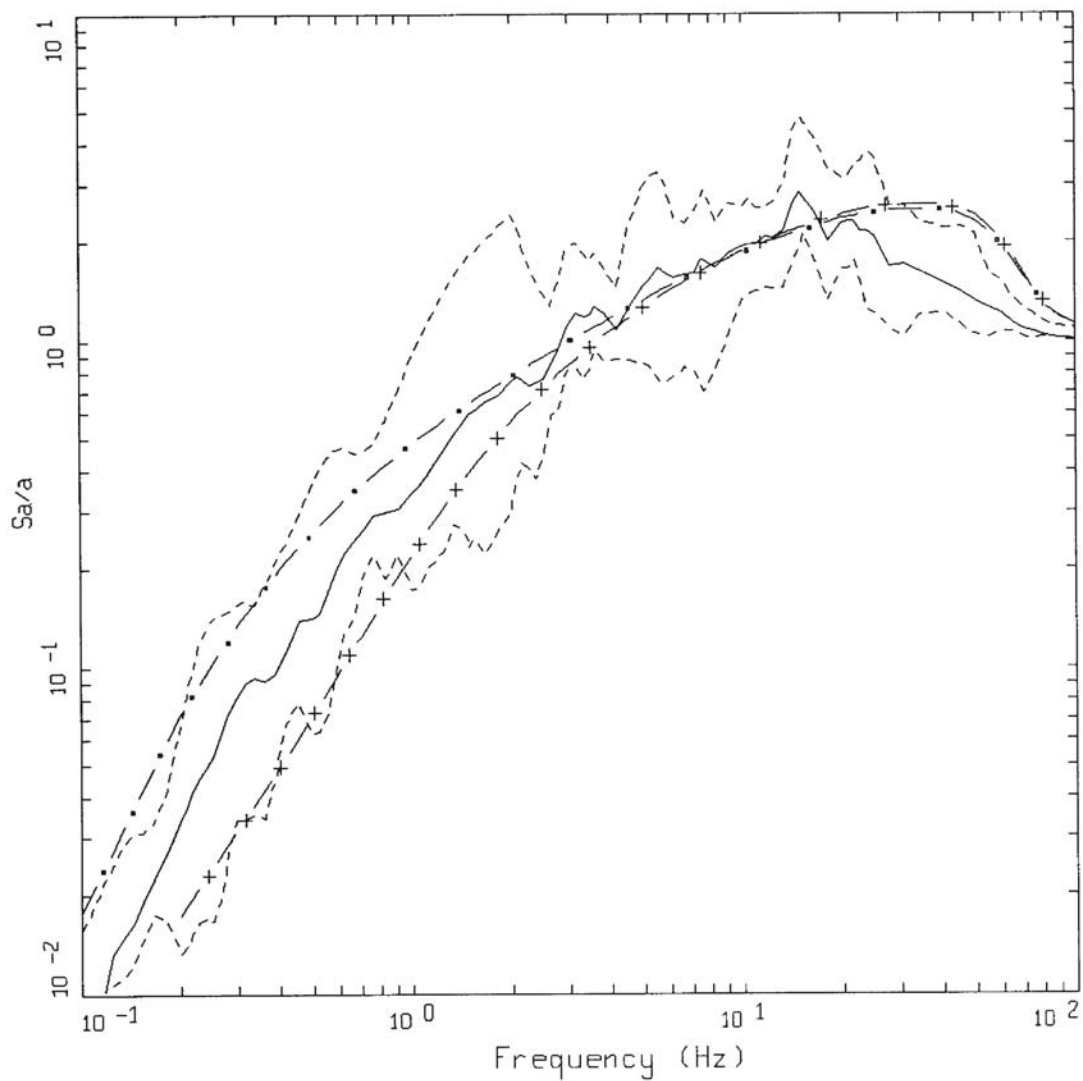
Figure C-9. Absolute response spectra (5% damping) computed for $M = 6.5$ at $R = 25$ km using both single and double corner frequency source spectra for WUS and CEUS conditions (Table C2).



AVERAGE HORIZONTAL SPECTRA, WUS
 M=6.75 (6.5-7.0), R=10-50 KM, ROCK
 AVERAGE M = 6.75, AVERAGE DISTANCE = 30.78 KM

- LEGEND
- 50TH PERCENTILE
 - - - - MINIMUM ENVELOPE
 - - - - MAXIMUM ENVELOPE
 - · - WUS SINGLE CORNER MODEL
 - + - WUS DOUBLE CORNER MODEL

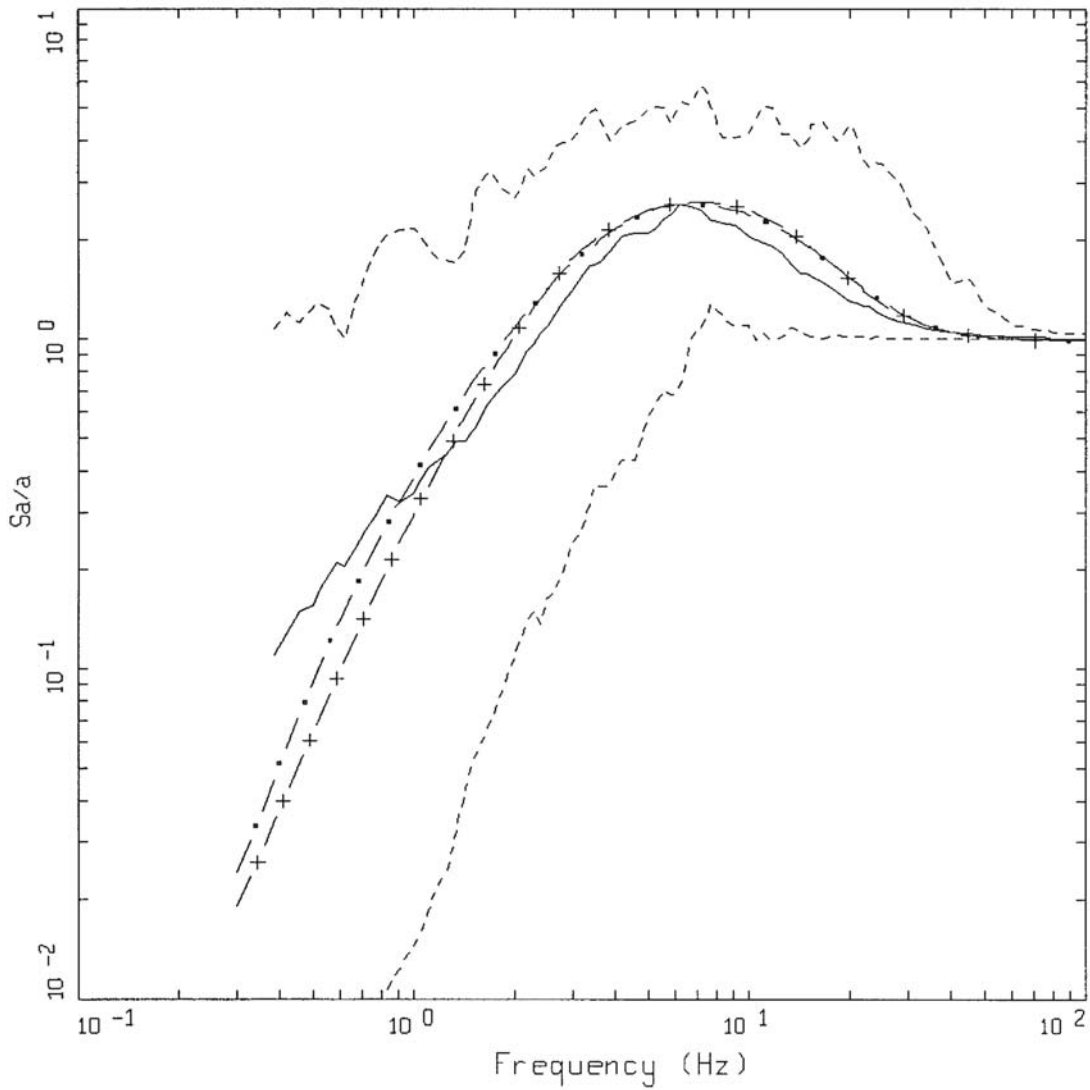
Figure C-10. Comparison of 5% damped statistical shapes computed for WUS recordings (M 6¼) to single and double corner model predictions using the parameters listed in Table C2.



AVERAGE HORIZONTAL SPECTRA, CEUS
 M=6.8, R=5-50 KM, ROCK

- LEGEND
- 50TH PERCENTILE
 - - - - MINIMUM ENVELOPE
 - - - - MAXIMUM ENVELOPE
 - · - CEUS SINGLE CORNER MODEL
 - + - CEUS DOUBLE CORNER MODEL

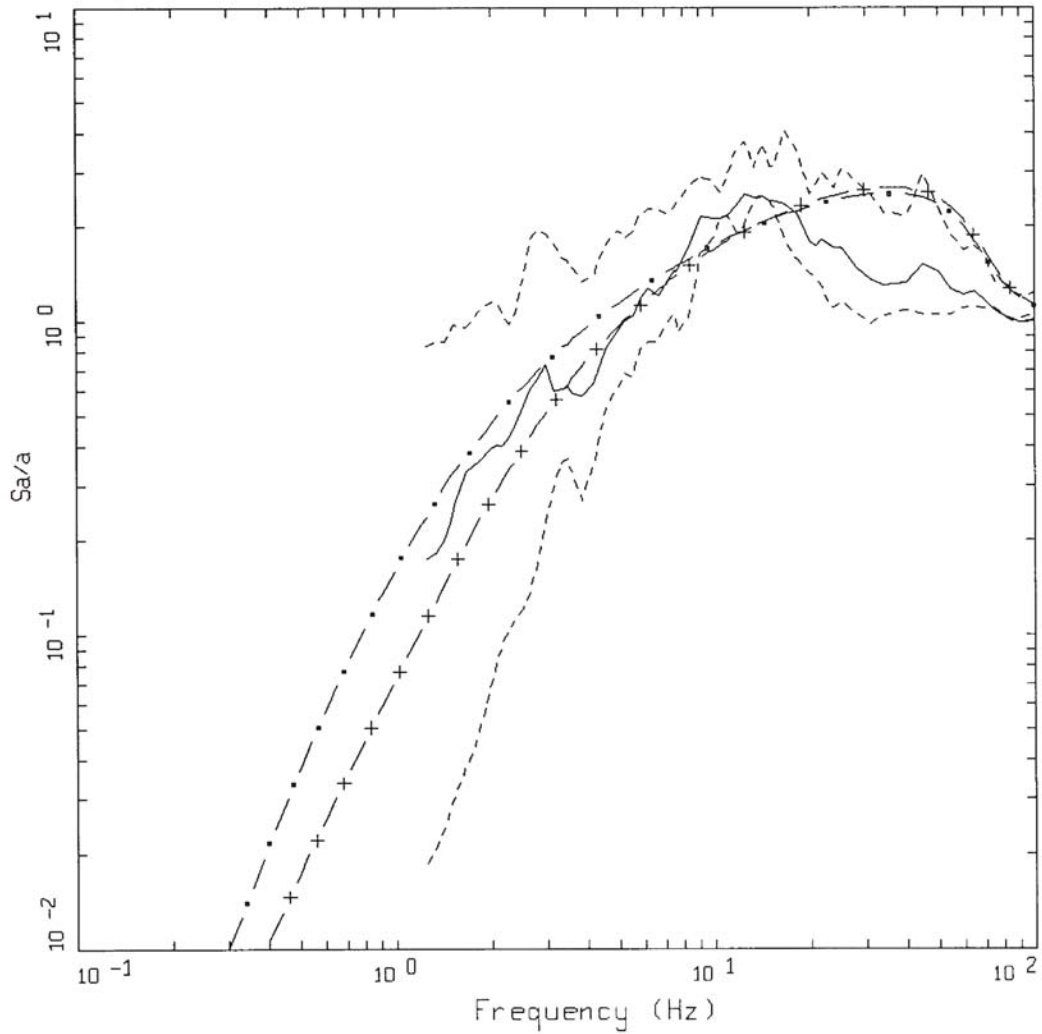
Figure C-11. Comparison of 5% damped statistical shapes computed for CEUS recordings ($M 6^{3/4}$) to single and double corner model predictions using the parameters listed in Table C2.



AVERAGE HORIZONTAL SPECTRA, WUS
 M=5 1/4 (5.0-5.4), R=0-25 KM, ROCK
 AVERAGE M = 5.18, AVERAGE DISTANCE = 13.57 KM

- LEGEND
- 50TH PERCENTILE
 - - - - MINIMUM ENVELOPE
 - · - · - MAXIMUM ENVELOPE
 - · - WUS SINGLE CORNER MODEL
 - + - WUS DOUBLE CORNER MODEL

Figure C-12. Comparison of 5% damped statistical shapes computed for WUS recordings (M 5¼) to single and double corner model predictions using the parameters listed in Table C2.



AVERAGE HORIZONTAL SPECTRA, CEUS
 $M=5 \frac{1}{4}$, $R=0-25$ KM, ROCK

- LEGEND
- 50TH PERCENTILE
 - - - MINIMUM ENVELOPE
 - - - MAXIMUM ENVELOPE
 - · - CEUS SINGLE CORNER MODEL
 - + - CEUS DOUBLE CORNER MODEL

Figure C-13. Comparison of 5% damped statistical shapes computed for CEUS recordings ($M 5 \frac{1}{4}$) to single and double corner model predictions using the parameters listed in Table C2.